

1           **An approach for modelling volume change of fine-grained soil**  
2   **subjected to thermal cycles**

3   **Authors:** Q. J. Ma\*, C. W. W. Ng, D. Mašín and C. Zhou

4   \*Corresponding author

5   **Information of the authors**

6   **Corresponding author:** Mr Q. J. Ma

7   Research student, Department of Civil and Environmental Engineering, Hong Kong University  
8   of Science and Technology, Clear Water Bay, Kowloon, Hong Kong.

9   E-mail: qmaah@connect.ust.hk

10   **Co-author:** Dr C. W. W. Ng

11   Chair Professor, Department of Civil and Environmental Engineering, Hong Kong University  
12   of Science and Technology, Clear Water Bay, Kowloon, Hong Kong.

13   E-mail: charles.ng@ust.hk

14   **Co-author:** Dr D. Mašín

15   Associate Professor, Faculty of Science, Charles University in Prague, Czech Republic.

16   E-mail: masin@natur.cuni.cz

17 **Co-author:** Dr C. Zhou

18 Visiting Assistant Professor, Department of Civil and Environmental Engineering, Hong Kong

19 University of Science and Technology, Clear Water Bay, Kowloon, Hong Kong.

20 E-mail: [czhou@connect.ust.hk](mailto:czhou@connect.ust.hk)

21 **Abstract:** In consequence of cyclic heating and cooling about the ambient temperature  
22 under drained conditions, normally consolidated and lightly over-consolidated fine-grained  
23 soils experience accumulation of irreversible volumetric contraction. Most existing thermo-  
24 mechanical models were developed for one heating-cooling cycle and are not suitable for  
25 multiple thermal cycles. An approach is proposed to simulate the volume change of fine-  
26 grained soil induced by thermal cycles. In the proposed approach, a thermal stabilization line  
27 is introduced to control the stabilized volumetric contraction under thermal cycles.  
28 Comparison with experimental results shows that the proposed approach can reproduce  
29 well the cumulative feature of volumetric contraction of fine-grained soil subjected to  
30 thermal cycles.  
31 *Key words:* thermal, cyclic, fine-grained soil, constitutive modelling.

## 32 **Introduction**

33 Thermal effects on soil behaviour have drawn attention from researchers throughout the  
34 past decades (Campanella & Mitchell, 1968; Leroueil & Marques, 1996; Hueckel et al., 2009;  
35 Gens, 2010). Under drained conditions, a monotonic temperature increase can induce  
36 irreversible volumetric contraction of normally consolidated (NC) and lightly over-  
37 consolidated (OC) fine-grained soils (e.g., Baldi et al., 1988; Sultan et al., 2002; Cekerevac &  
38 Laloui, 2004; Abuel-Naga et al., 2007; Uchaipichat & Khalili, 2009; Ng et al., 2016). When  
39 subjected to thermal cycles, irreversible volumetric contraction accumulates, and stabilizes  
40 within less than 5 thermal cycles (e.g., Campanella & Mitchell, 1968; Vega & McCartney,  
41 2014; Di Donna & Laloui, 2015). The accumulation of irreversible volume contraction with  
42 thermal cycles is likely due to the degradation of the inter-particle shear strength under  
43 elevated temperatures (Campanella & Mitchell, 1968; Di Donna & Laloui, 2015) and the soil  
44 creep (Leroueil & Marques, 1996; Vega & McCartney, 2014).

45 To model the thermally induced volume change of fine-grained soil, the critical state  
46 framework was extended incorporating the shrinkage of yield surface with increasing  
47 temperature (e.g., Hueckel & Baldi, 1990; Graham et al., 2001; Laloui & Cekerevac, 2003). In  
48 some other models (e.g., Cui et al., 2000; Abuel-Naga et al., 2007), an extra thermal yield  
49 surface was introduced to improve the simulation of over-consolidated soil. It should be

50 noted that these models simulate well one heating-cooling cycle, but cannot give the  
51 cumulative trend of irreversible volumetric contraction with thermal cycles. Although the  
52 thermo-mechanical models based on the concept of hypoplasticity can capture the  
53 cumulative trend (e.g., Mašin & Khalili, 2012; Zhou & Ng, 2015), they tend to overestimate  
54 the accumulated irreversible volumetric contraction. Di Donna & Laloui (2015) furthered the  
55 work by Laloui & François (2009) to account for cyclic thermal loading through modifying the  
56 rule governing the plasticity mobilization during cooling.

57 The accumulation and stabilization of irreversible volume contraction of fine-grained soil  
58 subjected to thermal cycles can be classified as a kind of shakedown (Collins & Boulbibane,  
59 2000). The concept of shakedown has been used to model the soil behaviour subjected to  
60 mechanical cyclic loading (e.g., Habiballah & Chazallon, 2005) and wetting-drying cycles  
61 (Nowamooz et al., 2016). Based on the concept of shakedown, an approach is proposed for  
62 simulating the volume change of fine-grained soil subjected to thermal cycles, with focus on  
63 NC soil. The sign convention used herein is in accordance with soil mechanics, positive for  
64 volume decrease and negative for volume increase.

## 65 **Proposed approach**

### 66 **Schematic illustration**

67 As suggested by the experimental results on soil volume change under thermal cycles (e.g.,

68 Campanella & Mitchell, 1968; Vega & McCartney, 2014; Di Donna & Laloui, 2015), a thermal  
69 stabilization line (TSL) is proposed, which controls the stabilized soil state under cyclic  
70 thermal loading. For simplicity, it is assumed to be a straight line in the  $\ln v - \ln p'$  space as  
71 shown in Fig. 1, where the normal compression line (NCL) and the thermal stabilization line  
72 (TSL) correspond to an elevated temperature. The point O represents the state of an NC soil  
73 specimen at the end of the first heating, and the point O' represents the stabilized state  
74 after several thermal cycles for the given temperature increase. The distance OO' reflects  
75 the accumulated irreversible volumetric contraction of the NC soil specimen after the first  
76 thermal cycle. If it equals 0, there is no accumulation of irreversible volumetric contraction.  
77 It is assumed that (1) As temperature changes the TSL shifts together with the NCL which is  
78 temperature dependent according to the experimental results (e.g., Campanella & Mitchell,  
79 1968); (2) During heating, if the soil state is above the current TSL there is heating induced  
80 irreversible volumetric contraction; Otherwise the soil response is thermo-elastic; (3) During  
81 cooling, the soil response is thermo-elastic. Admittedly, the influence of temperature on the  
82 TSL is difficult to experimentally quantify. It is a postulation made by the authors to fit best  
83 the available data. In addition, the effect of pre-consolidation pressure on the TSL is likely to  
84 be small. This is because experimental results from Abuel-Naga et al. (2007) show that the  
85 thermally induced volume change of soil is almost independent of the pre-consolidation  
86 pressure. Based on the assumptions, it can be deduced that if the distance OO' equals 0 and

87 the slope of the TSL equals that of the NCL, the proposed approach is reduced to that  
88 proposed by Hueckel & Baldi (1990) and Laloui & Cekerevac (2003).

89 Vega & McCartney (2014) carried out odometer tests on the volume change of saturated silt  
90 with different OCRs subjected to 4 thermal cycles (18 – 91 °C). The results are shown in Fig.  
91 2, where the open circle and solid circle represent the initial state and final state of the soil  
92 specimen, respectively. Although there are some discrepancies, the final stabilized states can  
93 be represented by the TSL proposed.

94 An NC soil specimen subjected to thermal cycles at constant effective stress is analysed to  
95 illustrate how the proposed approach works. Fig. 3 shows the state evolution of the NC soil  
96 specimen during thermal cycles. The open and solid circles represent the initial state and the  
97 current state of the soil specimen, respectively. The initial state means the soil state before  
98 the first thermal cycle. The dashed and solid lines correspond to the initial temperature  
99 ( $\Delta T = 0 \text{ }^\circ\text{C}$ ) and the elevated temperature ( $\Delta T > 0 \text{ }^\circ\text{C}$ ), respectively. During the first  
100 heating, both the NCL and the TSL shift downward, and the soil state stays on the NCL. Based  
101 on the experimental results (e.g., Abuel-Naga et al., 2007; Uchaipichat & Khalili, 2009), it is  
102 reasonable to assume that soil response is thermo-elastic during cooling. For traditional  
103 mechanical loading, the volume change is equivalent to the change of void ratio. However,  
104 the thermo-elastic soil deformation results in the change of soil volume, but not the void

105 ratio. This is because for thermo-elastic soil deformation the volume change of voids and soil  
106 particles is proportional to each other (Khalili et al., 2010; Mašín & Khalili, 2012). Therefore,  
107 during cooling the soil state remains unchanged while the NCL and TSL return back to their  
108 initial positions. Fig. 3(a) shows the soil state after the first thermal cycle. The corresponding  
109 soil response during the first thermal cycle is qualitatively represented by the curve in Fig.  
110 3(b), which shows a continuous irreversible volumetric contraction during heating and  
111 elastic response during cooling.

112 Upon re-heating, initially the soil state is below the TSL and the soil response is thermo-  
113 elastic according to the assumptions made previously. As temperature increases both the  
114 NCL and the TSL shift downward, with the TSL shifting more compared to the NCL. As the TSL  
115 crosses the soil state point, it attracts the soil state point to move downward. Therefore,  
116 there occurs more irreversible volumetric contraction. As stated in the introduction, the  
117 accumulation and stabilization of irreversible volumetric contraction with thermal cycles can  
118 be well characterized by the shakedown concept. According to the concept of shakedown,  
119 the soil specimen approaches the stabilized state after a certain number of cycles. Therefore,  
120 at the end of the second thermal cycle the soil state may stay slightly above the TSL (see Fig.  
121 3c), which controls the stabilized state of the soil subjected to thermal cycles. Compared to  
122 the state after the first thermal cycle (see Fig. 3a), the vertical distance  $\Delta \ln(1 + e)$  between  
123 the soil state point and the TSL is reduced. Qualitatively, the soil response during the second



124 thermal cycle is demonstrated by the curve in Fig. 3(d). At the beginning of heating, soil  
125 response is thermo-elastic and after temperature reaches some value it turns to be thermo-  
126 plastic. It is easy to predict that after several thermal cycles the soil state eventually  
127 approaches the TSL corresponding to the elevated temperature and the vertical distance  
128  $\Delta \ln(1 + e)$  decreases to zero as presented in Fig. 3(e). Thus, during subsequent heating  
129 there is no irreversible volumetric contraction if the temperature does not exceed the  
130 history maximum value. As shown in Fig. 3(f) the soil response turns to be stabilized  
131 corresponding to the given maximum temperature increase.

### 132 **Mathematical formulation**

133 According to Mašín & Khalili (2012), the temperature dependent NCLs can be expressed as

$$\ln(1 + e) = N(T) - \lambda(T) \cdot \ln(p'/p_r) \quad (1)$$

134 where  $e$  is the void ratio;  $p'$  is the mean effective stress;  $p_r$  is the reference pressure (1 kPa);

135  $\lambda(T)$  and  $N(T)$  are the temperature dependent slope and intercept of the NCL, respectively.

136 They are assumed to follow

$$N(T) = N(T_r) + n_T \cdot \ln(T/T_r) \quad (2)$$

$$\lambda(T) = \lambda(T_r) + l_T \cdot \ln(T/T_r) \quad (3)$$

137 where  $n_T$  and  $l_T$  are model parameters controlling the shift and slope change of the NCL

138 with temperature, respectively;  $T_r$  is the reference temperature. According to the

139 experimental results (e.g., Campanella & Mitchell, 1968), it is assumed that  $\lambda$  is independent  
140 of temperature, and thus  $l_T$  can be chosen as 0.

141 The newly introduced TSL is determined by its slope  $k_T$  and the point  $O'$  as shown in Fig. 1. It  
142 is expressed by

$$\ln(1 + e) = \ln(1 + e_{o'}) - k_T \cdot \ln(p'/p'_o) \quad (4)$$

143 where  $p'_o$  is the pre-consolidation pressure;  $\ln(1 + e_{o'})$  can be calculated from

$$\ln(1 + e_{o'}) = \ln(1 + e_o) + c_T \cdot n_T \cdot \ln(T/T_r) \quad (5)$$

144 where  $e_o$  and  $e_{o'}$  represent the void ratio corresponding to point O and point  $O'$ ,  
145 respectively. If the temperature is lower than the reference temperature,  $e_{o'}$  is assumed to  
146 be equal to  $e_o$ .

147 The newly introduced parameter  $c_T$  determines the accumulated volumetric contraction  
148 after the first thermal cycle. If it equals 0, there is no accumulation. The slope parameter  $k_T$   
149 influences the simulated irreversible volumetric contraction of OC soil. As  $k_T$  decreases, the  
150 simulated irreversible volumetric contraction of OC soil increases as it is more likely for the  
151 TSL to cross the soil state point during heating.

## 152 **Implementation of the proposed approach**

### 153 **Implementation**

154 The proposed approach is combined with the hypoplastic framework. The basic hypoplastic  
 155 model for fine-grained soil developed by Mašín (2005) takes a nonlinear relationship  
 156 between the Jaumann stress rate tensor  $\dot{\boldsymbol{\sigma}}$  and the Euler strain rate tensor  $\dot{\boldsymbol{\varepsilon}}$  as

$$\dot{\boldsymbol{\sigma}} = f_s(\mathcal{L} : \dot{\boldsymbol{\varepsilon}} + f_d \mathbf{N} \|\dot{\boldsymbol{\varepsilon}}\|) \quad (6)$$

157 where  $\mathcal{L}$  and  $\mathbf{N}$  are fourth-order and second-order constitutive tensors, respectively;  $f_s$  and  
 158  $f_d$  are scalar factors to consider the effects of stress level and void ratio, respectively;  $:$   
 159 stands for double contraction and  $\|\mathbf{X}\|$  denotes the Euclidean norm of the tensor  $\mathbf{X}$ . Detailed  
 160 mathematical expressions and discussions of the terms involved can be found in Mašín  
 161 (2005).

162 To model thermally-induced volume change of soil, Mašín & Khalili (2012) introduced a  
 163 thermal term  $f_u \mathbf{H}_T$  into Eq. 6 as

$$\dot{\boldsymbol{\sigma}} = f_s[\mathcal{L} : (\dot{\boldsymbol{\varepsilon}} - \dot{\boldsymbol{\varepsilon}}^{\text{TE}}) + f_d \mathbf{N} \|\dot{\boldsymbol{\varepsilon}} - \dot{\boldsymbol{\varepsilon}}^{\text{TE}}\|] + f_u \mathbf{H}_T \quad (7)$$

164  $\dot{\boldsymbol{\varepsilon}}^{\text{TE}}$  is the isotropic thermo-elastic strain rate tensor and calculated by

$$\dot{\boldsymbol{\varepsilon}}^{\text{TE}} = \frac{1}{3} \alpha_s \cdot \dot{T} \cdot \mathbf{I} \quad (8)$$

165 where  $\alpha_s$  is the volumetric thermal expansion coefficient of soil skeleton and  $\dot{T}$  is the  
 166 temperature change rate.  $\mathbf{I}$  is the second order unit tensor. The thermal part is coupled with  
 167 the mechanical part through the void ratio, which influences the soil behaviour under both

168 thermal and mechanical loading. In addition, thermal loading can change the size of the  
169 state boundary surface (Eqs. 1-2), and thus affect the soil behaviour under mechanical  
170 loading. Also, mechanical loading changes the size of the state boundary surface, which  
171 affects the thermal response for states at or close to the state boundary surface.

172 The mathematical expression for  $H_T$  was derived by considering that when subjected to  
173 heating at constant effective stress, the NC soil stays on the NCL as it moves with  
174 temperature change (Mašín & Khalili, 2012). The collapse potential factor  $0 \leq f_u \leq 1$   
175 controls the heating induced irreversible volumetric contraction. The larger the collapse  
176 potential factor  $f_u$  the more irreversible volumetric contraction heating can induce. For an  
177 NC soil specimen during the first heating  $f_u$  equals 1. When  $f_u$  equals 0 it implies the soil  
178 response is thermo-elastic.

179 To implement the proposed approach within the hypoplastic framework, the key point lies in  
180 modifying the collapse potential factor  $f_u$ , which controls the thermally induced irreversible  
181 volumetric contraction of soil. Its expression should satisfy two requirements: (1) the NC soil  
182 stays on the NCL during the first heating; (2) as the soil state approaches the TSL the collapse  
183 potential decreases to zero. The revised expression is expressed as Eq. 9

$$f_u = \left\langle \frac{e - e_T^*}{e_T - e_T^*} \right\rangle^\gamma \quad (9)$$

184 where  $\langle x \rangle$  is an operator obtaining the positive part of the scalar variable  $x$ ,  $\langle x \rangle =$   
185  $(x + |x|)/2$ ;  $e$  is the void ratio;  $e_T$  and  $e_T^*$  are the void ratios on the current NCL and TSL  
186 corresponding to the current mean effective stress, respectively (see point C in Fig. 1). They  
187 can be calculated from Eq. (1) and (4), respectively.  $\gamma$  is a new parameter controlling the rate  
188 of irreversible volumetric contraction development with respect to the heating rate. As a  
189 consequence, it controls the number of thermal cycles required to get the soil volumetric  
190 contraction stabilized.

#### 191 **Calibration of model parameters**

192 In this section, calibration of the three newly introduced parameters  $c_T$ ,  $k_T$  and  $\gamma$  is  
193 discussed. For the calibration of other relevant model parameters, please refer to Mašín  
194 (2005) and Mašín & Khalili (2012). To calibrate the parameter  $c_T$ , a volume change test of an  
195 NC soil specimen subjected to thermal cycles until stabilization is required. Regarding the  
196 slope parameter  $k_T$ , test results of soil specimens with different OCRs are necessary. It can  
197 be determined based on the threshold value of OCR corresponding to which there is no  
198 heating induced irreversible volumetric contraction for a given temperature increase. The  
199 crossing point of the thermal stabilization line for the given temperature increase and the  
200 unloading line corresponds to the threshold OCR. Ideally, experiments are required to  
201 calibrate the two parameters. However, performing cyclic thermal loading test could be very

202 complex and time consuming. Based on the published experimental results (Campanella &  
203 Mitchell, 1968; Vega & McCartney, 2014; Di Donna & Laloui, 2015), a value between 0.4 and  
204 0.5 is suggested for the parameter  $c_T$ . Regarding the parameter  $k_T$  values from 0.01 to 0.015  
205 calibrated in this work can be adopted for simulations as a starting point. It should be noted  
206 that  $k_T$  is supposed to be larger than the unloading parameter  $\kappa$  (see Figs. 1 & 2). The  
207 thermal parameters adopted in this study are determined by back-analysing the  
208 experimental results, and best agreement is achieved through trial and error.

209 A sensitivity analysis was conducted to study the effect of the parameter  $\gamma$  on the  
210 accumulation of irreversible volumetric contraction of an NC soil specimen with thermal  
211 cycles. Model parameters used are these for the soil tested by Uchaipichat & Khalili (2009)  
212 (see Table 1). The four parameters  $\varphi_c$ ,  $\lambda$ ,  $\kappa$  and  $N$  of the mechanical part in Table 1 are the  
213 same as those for the critical state theory. The parameter  $r$  controls the ratio of shear  
214 stiffness to bulk stiffness. Obtained results are shown in Fig. 4, which indicates that as  $\gamma$   
215 decreases the soil volumetric contraction stabilizes within less number of thermal cycles.  
216 Specifically, for  $\gamma = 0.1$  it stabilizes around the fifth thermal cycle, which is consistent with  
217 the experimental results (e.g., Vega & McCartney, 2014). Based on the sensitivity analysis, a  
218 default value of 0.1 is suggested for  $\gamma$ . It should be noted that the parameter  $\gamma$  does not  
219 affect the irreversible volumetric contraction corresponding to the first thermal cycle. For an  
220 NC soil specimen during the first heating, the soil state remains on the NCL, and thus its

221 volumetric contraction is completely determined by the parameter  $n_T$  which controls the  
222 shift of NCL with temperature increase (see Eq. 2).

### 223 **Typical results**

224 Fig. 5 presents the computed volume change of soil specimens with 4 different OCRs (1, 1.3,  
225 2 and 4) subjected to 15 thermal cycles (25 – 60 °C) using model parameters for the soil  
226 tested by Uchaipichat & Khalili (2009) (see Table 1). It can be seen that as the OCR increases,  
227 both the irreversible volumetric contraction after the first thermal cycle and that  
228 corresponding to the stabilized state decrease. For all the soil specimens the irreversible  
229 volumetric contraction stabilizes within roughly five thermal cycles. For the soil specimen  
230 with OCR of 4, there is no irreversible volumetric contraction, which indicates a thermo-  
231 elastic soil response. It can be predicted that for soil specimen with even higher OCRs, the  
232 simulated soil response is also going to be thermo-elastic. These trends are in good  
233 agreement with experimental results of saturated silt with different OCRs from Vega &  
234 McCartney (2014).

### 235 **Evaluation of the proposed approach**

236 Experimental test of remoulded illite from Campanella & Mitchell (1968) was simulated  
237 using the newly proposed approach and the approach proposed by Mašín & Khalili (2012)  
238 for comparison. The soil specimen was consolidated under isotropic condition to 200 kPa.

239 Then three heating-cooling cycles (from about 60 °C to 5 °C) were applied under drained  
240 conditions at constant mean effective stress. The initial temperature of the soil specimen  
241 was around 20 °C. Adopted model parameters are summarized in Table 1.

242 Fig. 6(a) compares the experimental results with that computed using the model proposed  
243 by Mašín & Khalili (2012). It is clear that, compared to the measured results, the model  
244 predicts excessive accumulation of irreversible volumetric contraction with thermal cycles.

245 Comparison of the experimental results and the computed results from the newly proposed  
246 approach is shown in Fig. 6(b). Overall, it shows a reasonably good correlation between  
247 them, and the excessive accumulation is well avoided. The irreversible volumetric  
248 contraction accumulates at a decreasing rate. The temperature at which irreversible  
249 volumetric contraction occurs increases cycle after cycle. It should be noted that the  
250 proposed approach has some limitation in simulating the nonlinearity during the cooling and  
251 initial re-heating process. The adopted elastic assumption during cooling and initial re-  
252 heating is for simplicity. Actually, published results show somehow contradictory trend  
253 during the cooling and initial re-heating process (e.g., Campanella & Mitchell, 1968 and Ng  
254 et al., 2016). Therefore, more research is certainly required to confirm the trend  
255 experimentally and then improve the approach further.

## 256 **Summary**



257 Based on the experimental results, a thermal stabilization line is introduced in the  $\ln v - \ln p'$   
258 space, which controls the stabilized soil state under cyclic thermal loading. Two parameters  
259 are needed to characterize the thermal stabilization line. One determines the accumulated  
260 irreversible volumetric contraction for an NC soil specimen, and the other influences the  
261 simulated results of OC soil. By taking use of the introduced thermal stabilization line, a  
262 method is proposed to model the volume change of fine-grained soil subjected to thermal  
263 cycles. The proposed method is realized within the hypoplastic framework and tested  
264 against experimental results. The comparison shows that the proposed method is able to  
265 simulate the overall trend of accumulation and stabilization of irreversible volumetric  
266 contraction with thermal cycles.

## 267 **Acknowledgements**

268 The first author greatly appreciates the HKPFS scholarship offered by the Research Grants  
269 Council (RGC) of the HKSAR. The financial support provided by the RGC of the HKSAR (grant  
270 no. GRF 617213 and 16209415), the HKUST (grant no. FP204) and the National Science  
271 Foundation of China (grant no. 51378178) are also gratefully acknowledged.

## 272 **References**

273 Abuel-Naga, H. M., Bergado, D. T., Bouazza, A. & Ramana, G. V. 2007. Volume change  
274 behaviour of saturated clays under drained heating conditions: experimental results

275 and constitutive modelling. *Canadian Geotechnical Journal*, **44**(8): 942–956. doi:  
276 10.1139/t07-031.

277 Baldi, G., Hueckel, T. & Pellegrini, R. 1988. Thermal volume changes of the mineral-water  
278 system in low-porosity clay soils. *Canadian Geotechnical Journal*, **25**(4): 807–825. doi:  
279 10.1139/t88-089.

280 Campanella, R. G. & Mitchell, J. K. 1968. Influence of temperature variations on soil behavior.  
281 *Journal of the Soil Mechanics and Foundations Division, ASCE* **94**(3): 709–734.

282 Cekerevac, C. & Laloui, L. 2004. Experimental study of thermal effects on the mechanical  
283 behaviour of a clay. *International journal for numerical and analytical methods in*  
284 *geomechanics*, **28**(3): 209-228. doi: 10.1002/nag.332.

285 Collins, I. F. & Boulbibane, M. 2000. Geomechanical analysis of unbound pavements based  
286 on shakedown theory. *Journal of Geotechnical and Geoenvironmental Engineering*,  
287 **126**(1): 50-59. doi: 10.1061/(ASCE)1090-0241(2000)126:1(50).

288 Cui, Y. J., Sultan, N. & Delage, P. 2000. A thermomechanical model for saturated clays.  
289 *Canadian Geotechnical Journal*, **37**(3): 607–620. doi: 10.1139/t99-111.

290 Di Donna, A. & Laloui, L. 2015. Response of soil subjected to thermal cyclic loading:  
291 experimental and constitutive study. *Engineering Geology*, **190**: 65–76. doi:

292 10.1016/j.enggeo.2015.03.003.

293 Gens, A. 2010. Soil–environment interactions in geotechnical engineering. *Géotechnique*,  
294 **60**(1): 3–74. doi: 10.1680/geot.9.P.109.

295 Graham, J., Tanaka, N., Crilly, T. & Alfaro, M. 2001. Modified Cam-Clay modelling of  
296 temperature effects in clays. *Canadian Geotechnical Journal*, **38**(3): 608–621. doi:  
297 10.1139/t00-125.

298 Habiballah, T. & Chazallon, C. 2005. An elastoplastic model based on the shakedown concept  
299 for flexible pavements unbound granular materials. *International Journal for Numerical  
300 and Analytical Methods in Geomechanics*, **29**(6): 577-596. doi: 10.1002/nag.426.

301 Hueckel, T. & Baldi, G. 1990. Thermoplasticity of Saturated Clays: Experimental Constitutive  
302 Study. *Journal of Geotechnical Engineering*, **116**(12): 1778–1796. doi:  
303 10.1061/(ASCE)0733-9410(1990)116:12(1778).

304 Hueckel, T., François, B. & Laloui, L. 2009. Explaining thermal failure in saturated clays.  
305 *Géotechnique*, **59**(3): 197-212. doi: 10.1680/geot.2009.59.3.197.

306 Khalili, N., Uchaipichat, A. & Javadi, A. A. 2010. Skeletal thermal expansion coefficient and  
307 thermo-hydro-mechanical constitutive relations for saturated homogeneous porous  
308 media. *Mechanics of materials*, **42**(6): 593-598. doi: 10.1016/j.mechmat.2010.04.001.

309 Laloui, L. & Cekerevac, C. 2003. Thermo-plasticity of clays: an isotropic yield mechanism.  
310 Computers and Geotechnics, **30**(8): 649–660. doi: 10.1016/j.compgeo.2003.09.001.

311 Laloui, L. & François, B. 2009. ACMEG-T: soil thermoplasticity model. Journal of engineering  
312 mechanics, **135**(9): 932-944. doi: 10.1061/(ASCE)EM.1943-7889.0000011.

313 Leroueil, S. & Marques, M.E.S. 1996. Importance of strain rate and temperature effects in  
314 geotechnical engineering. In Measuring and modeling time-dependent soil behavior.  
315 Edited by T.C. Sheahan and V.N. Kaliakin. Geotechnical Special Publication 61, ASCE,  
316 New York. pp. 1–60.

317 Mašín, D. & Khalili, N. 2012. A thermo-mechanical model for variably saturated soils based  
318 on hypoplasticity. International journal for numerical and analytical methods in  
319 geomechanics, **36**(12): 1461–1485. doi: 10.1002/nag.1058.

320 Mašín, D. 2005. A hypoplastic constitutive model for clays. International journal for  
321 numerical and analytical methods in geomechanics, **29**(4): 311–336. doi:  
322 10.1002/nag.416.

323 Ng, C. W. W., Cheng, Q., Zhou, C. & Alonso, E. E. 2016. Volume changes of an unsaturated  
324 clay during heating and cooling. Géotechnique Letters, **6**(3): 1-7. doi:  
325 10.1680/jgele.16.00059.

326 Nowamooz, H., Li, K. & Chazallon, C. 2016. Shakedown modeling of unsaturated expansive  
327 soils subjected to wetting and drying cycles. In E3S Web of Conferences, EDP Sciences.  
328 **9**: 08007. doi: 10.1051/e3sconf/20160908007.

329 Sultan, N., Delage, P. & Cui, Y. J. 2002. Temperature effects on the volume change behaviour  
330 of Boom clay. *Engineering Geology*, **64**(2): 135–145. doi: 10.1016/S0013-  
331 7952(01)00143-0.

332 Towhata, I., Kuntiwattanakul, P., Seko, I. and Ohishi, K. 1993. Volume change of clays induced  
333 by heating as observed in consolidation tests. *Soils and Foundations*, **33**(4): 170–183.  
334 doi: 10.3208/sandf1972.33.4\_170.

335 Uchaipichat, A. & Khalili, N. 2009. Experimental investigation of thermo-hydro-mechanical  
336 behaviour of an unsaturated silt. *Géotechnique*, **59**(4): 339-353. doi:  
337 10.1680/geot.2009.59.4.339.

338 Vega, A. & McCartney, J. S. 2014. Cyclic heating effects on thermal volume change of silt.  
339 *Environmental Geotechnics*, **2**(5): 257–268. doi: 10.1680/envgeo.13.00022.

340 Zhou, C. & Ng, C. W. W. 2015. A thermomechanical model for saturated soil at small and  
341 large strains. *Canadian Geotechnical Journal*, **52**(8): 1101–1110. doi: 10.1139/cgj-2014-  
342 0229.

## Tables and Figures

### List of tables

**Table 1.** A summary of model parameters.

### List of figures

**Fig. 1.** Concept of the newly proposed thermal stabilization line (TSL).

**Fig. 2.** Validation of the proposed thermal stabilization line (TSL) by experimental results from Vega & McCartney (2014).

**Fig. 3** Schematic illustration of the proposed approach for simulating volume change of an NC soil specimen subjected to thermal cycles with a constant amplitude: (a) soil state after the first thermal cycle; (b) soil response during the first thermal cycle; (c) soil state after the second thermal cycle; (d) soil response during the second thermal cycle; (e) soil state after stabilization; (f) soil response after stabilization.

**Fig. 4.** Effect of the parameter  $\gamma$  on simulated volume change of an NC soil specimen subjected to thermal cycles.

**Fig. 5.** Typical results of volume change of soil specimens with different OCRs subjected to thermal cycles from the newly proposed approach.

**Fig. 6.** Comparison of measured and computed results: (a) computed results from the approach proposed by Mašín & Khalili (2012); (b) computed results from the newly proposed approach.

**Table 1.** A summary of model parameters.

Soil tested by	Soil type	Mechanical part					Thermal part						
		$\varphi_c$ (°)	$\lambda$	$\kappa$	$N$	$r$	$h_T$	$n_T$	$\alpha_s$ (°C <sup>-1</sup> )	$T_r$ (°C)	$k_T$	$c_T$	$\gamma$
Uchaipichat & Khalili (2009)	Silt	29.5	0.06	0.002	0.772	0.2	0	-0.01	$3.5 \times 10^{-5}$	25	0.01	0.5	0.1
Campanella & Mitchell (1968)	Clay	22	0.092	0.027	1.178	Nil*	0	-0.009	$3.5 \times 10^{-5}$	20	Nil*	0.4	0.1

\* This parameter is irrelevant to the simulations conducted in this study.

**FIGURE 1** Concept of the newly proposed thermal stabilization line (TSL).

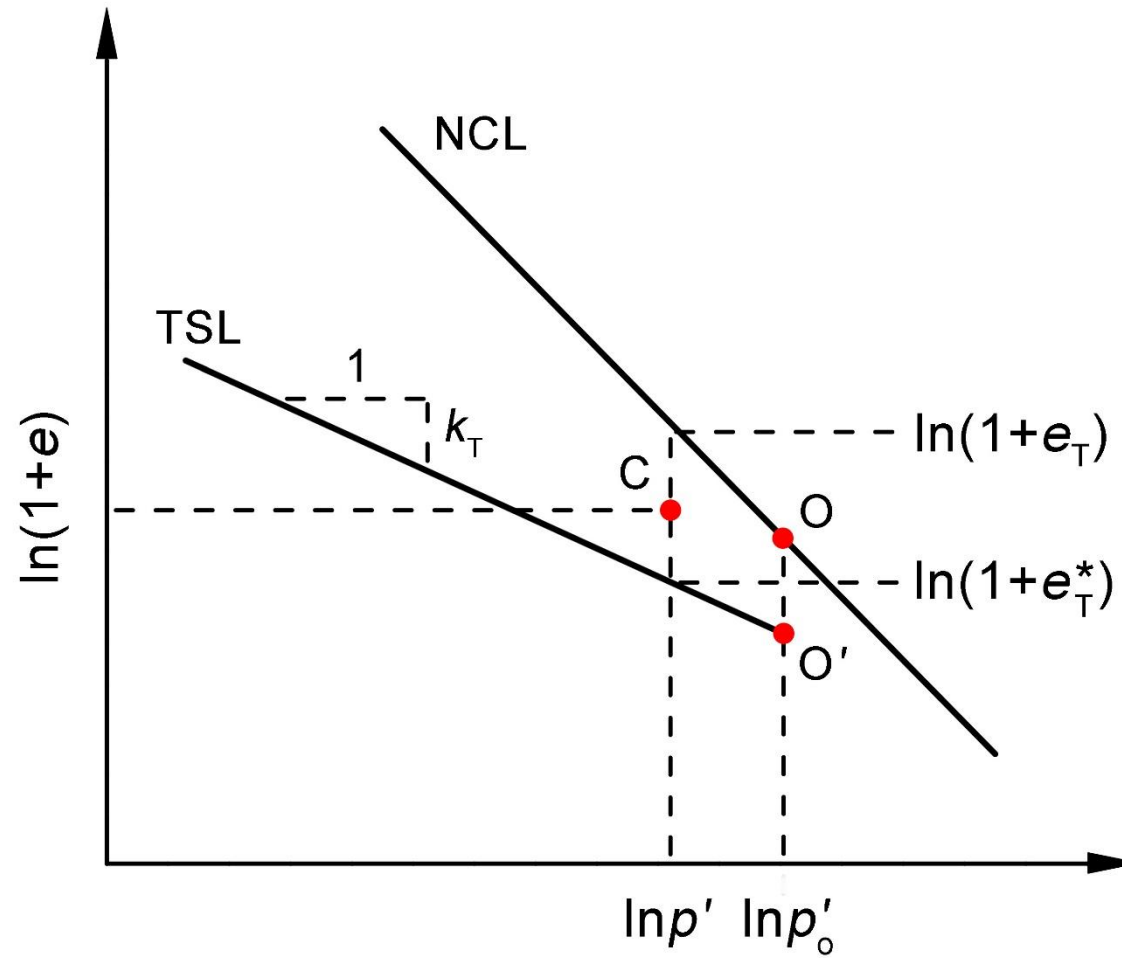




**FIGURE 2** Validation of the proposed thermal stabilization line (TSL) by experimental results from Vega & McCartney (2014).

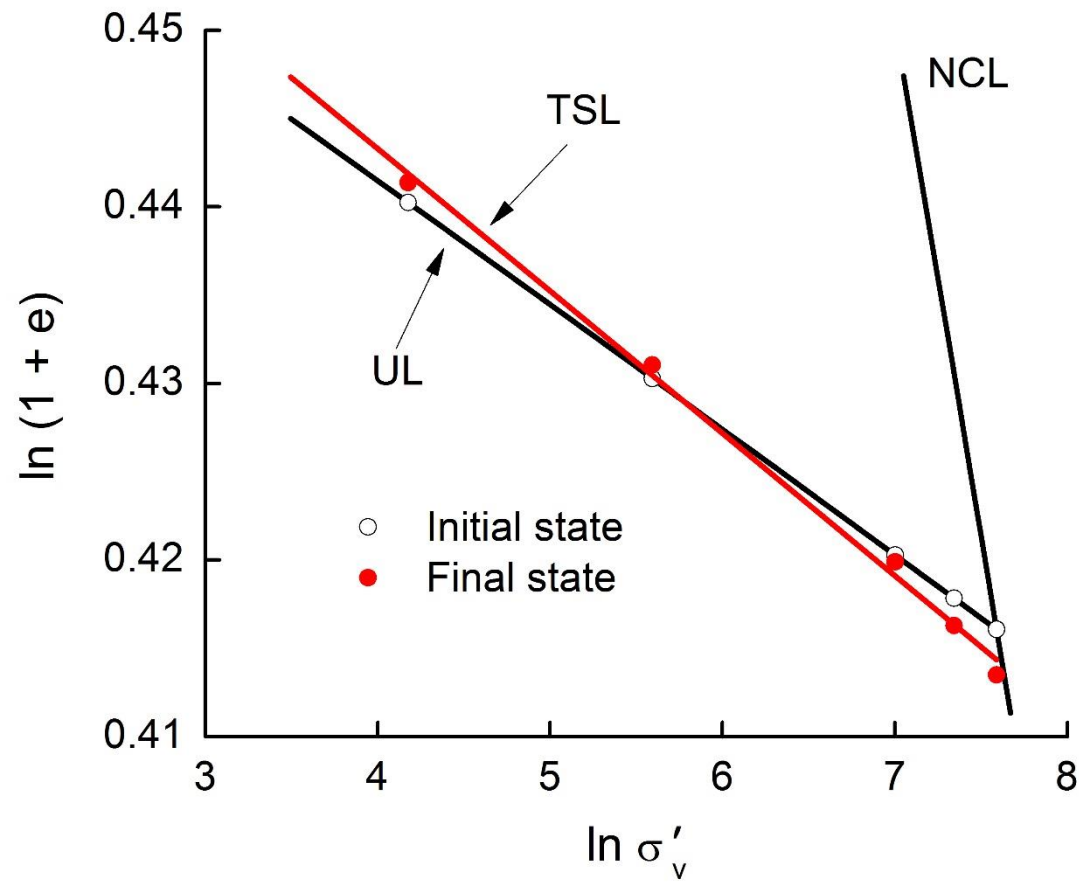


**FIGURE 3** Schematic illustration of the proposed approach for simulating volume change of an NC soil specimen subjected to thermal cycles with a constant amplitude: (a) soil state after the first thermal cycle; (b) soil response during the first thermal cycle; (c) soil state after the second thermal cycle; (d) soil response during the second thermal cycle; (e) soil state after stabilization; (f) soil response after stabilization.

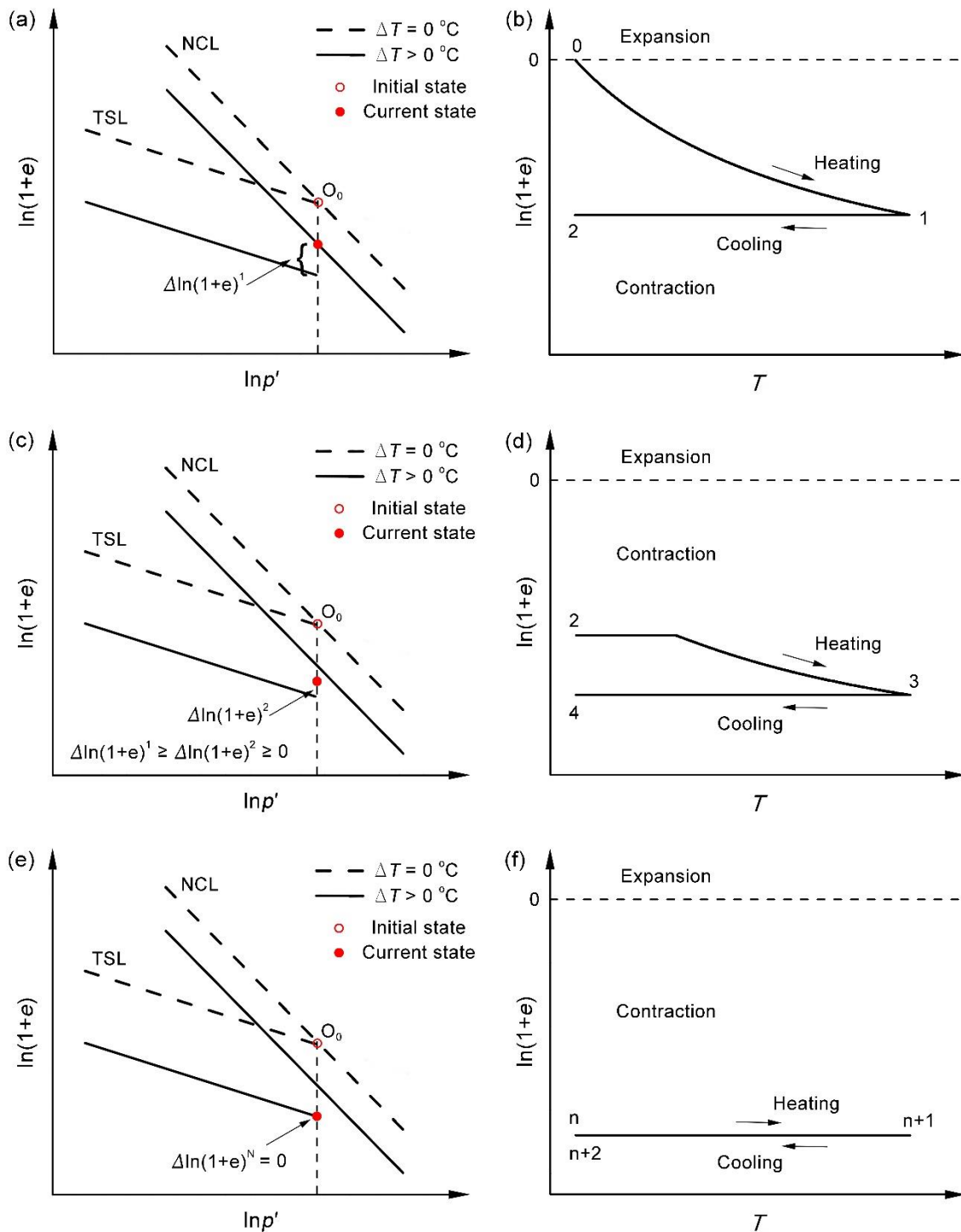


**FIGURE 4** Effect of the parameter  $\gamma$  on simulated volume change of an NC soil specimen subjected to thermal cycles.

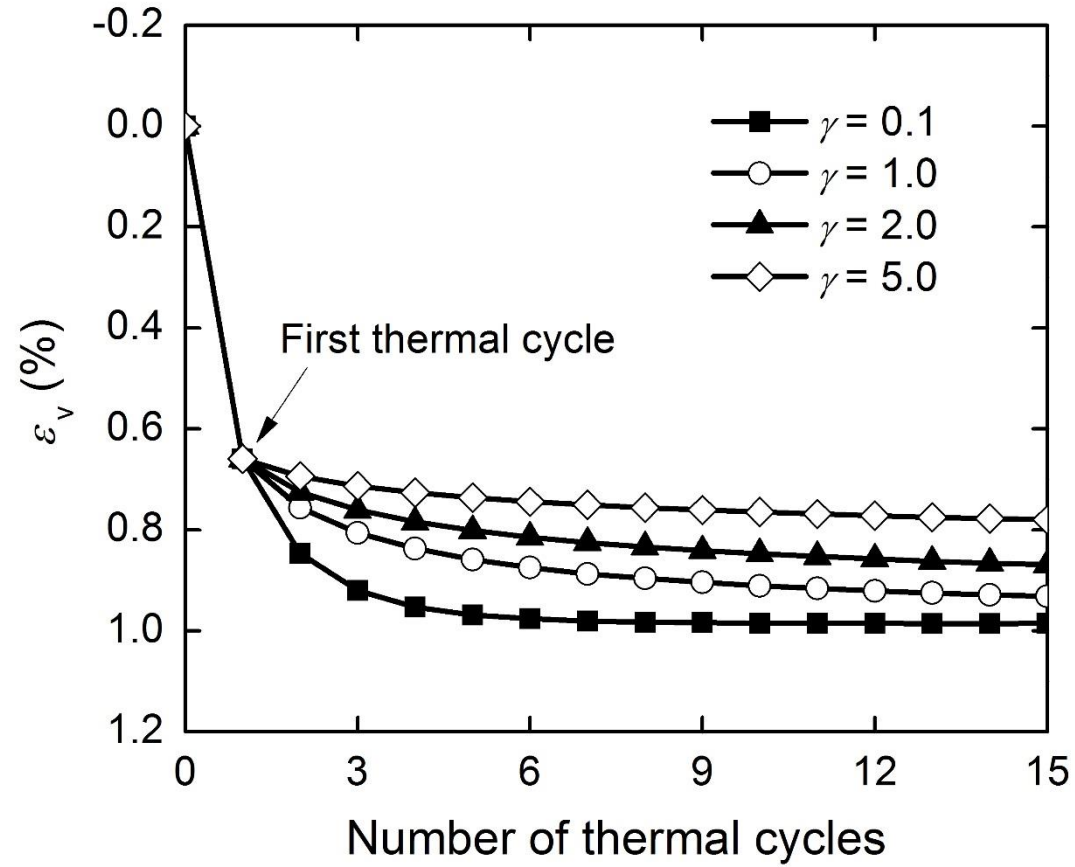


**FIGURE 5** Typical results of volume change of soil specimens with different OCRs subjected to thermal cycles from the newly proposed approach.

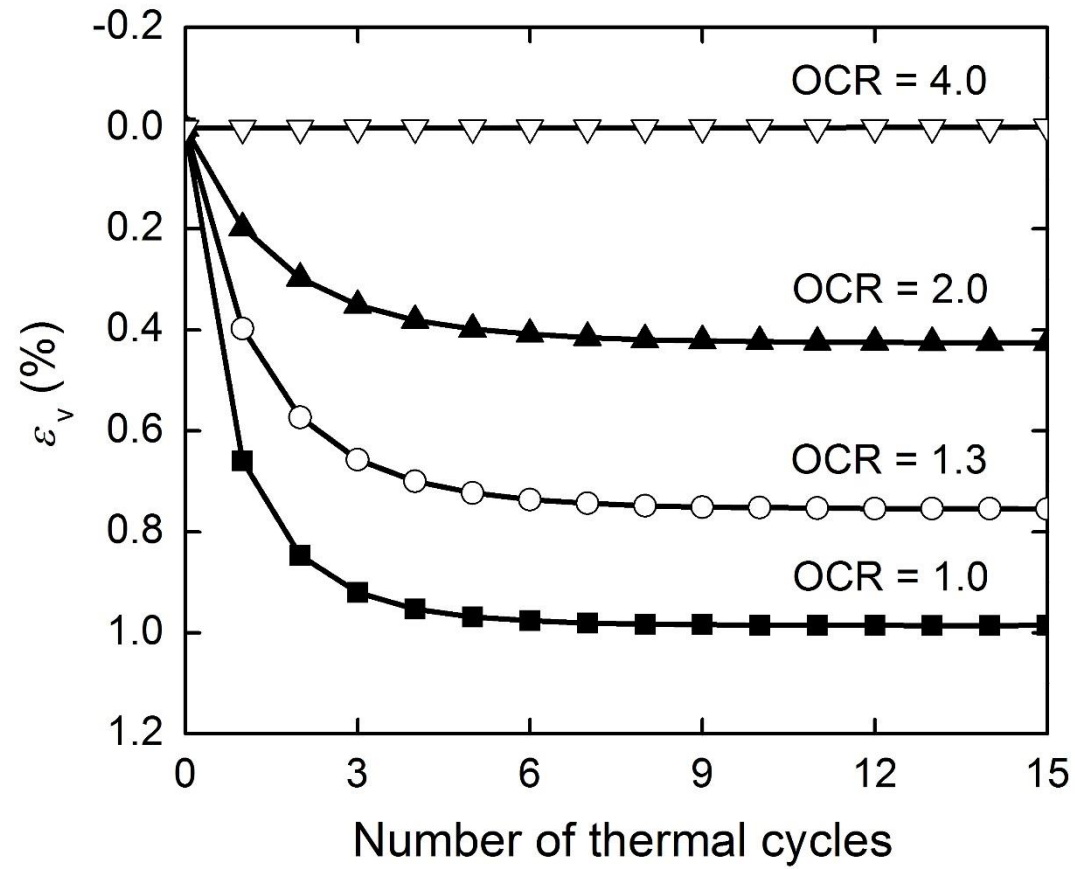


**FIGURE 6** Comparison of measured and computed results: (a) computed results from the approach proposed by Mašin & Khalili (2012); (b) computed results from the newly proposed approach.

